EXPERIMENTAL AND COMPUTATIONAL ANALYSIS OF A UAV FOR SUPERFICIAL VOLCANO SURVEILLANCE

Pedro David Bravo-Mosquera*, Laura Botero-Bolivar*, Daniel Acevedo-Giraldo*, Hernán Darío Cerón-Muñoz*, Fernando Martini Catalano*

* **Department of Aeronautical Engineering, São Carlos Engineering School, University of São Paulo, Brazil**

Keywords: *UAV, Conceptual design, CFD, Wind tunnel, LSB.*

Abstract

Nowadays, unmanned Aerial Vehicles (UAVs) technology has been improved considerably due to their ideal characteristic to recognize areas of difficult access, performing missions that could not be made with traditional manned aircraft. This work presents the experimental and computational analysis of a UAV for superficial volcano monitoring. The aerial vehicle, called URCUNINA-UAV aims to monitor the Galeras Volcano located in Colombia. The conceptual design of the aircraft is based on the design requirements established from a mission analysis. Computational Fluid Dynamics (CFD) simulations were done using Ansys-CFX. Experimental analysis was carried out in both open and closed wind tunnels in order to study all the possible aerodynamic phenomena that could be presented in the UAV mission. A Laminar Separation Bubble (LSB) was observed on the upper surface of the wing, which modify the aircraft performance considerably. However, the bubble formation was avoided using several transition processes. On the other hand, results showed that the entire design process was consistent because the numerical and experimental results were greatly similar in the aerodynamic coefficients. This suggested that the URCUNINA-UAV is potentially able to perform the proposed mission.

1 General Introduction

In the last decades, the study about design and optimization of Unmanned Aerial Vehicles (UAVs) has increased due to wide variety of applications, such as observation and surveys of ozone layer, polar zones, hurricane generation, tornado formation, power lines monitoring, among others [1]. However, in case of volcanic monitoring, the information about UAVs to perform this kind of mission is very limited. Usually, specialized research centers in volcanic eruptions have developed different procedures for analyzing the behavior inside and outside the craters. One of these procedures involves performing continuous flights over the volcanic domes, with the intervention of manned aircraft, i.e. the aircraft are equipped with instruments for in situ analysis the geographical, chemical and thermal changes over the volcano surfaces. However, the highly unfavourable flight conditions can affect the aircraft performance, risking the lives of the crew aboard [2-4]. Under these limitations, the removal of the crew from the aircraft, combined with remote sensing technology of UAVs appears as a viable solution to these issues.

In the present article is reported the design methodology of a UAV named URCUNINA (meaning Fire Mountain), whose mission is to perform flights around volcanoes, as well as its numerical analysis and wind tunnel tests.

In-depth exploration of the operational field of the URCUNINA-UAV was performed, aiming

to identify the Design Requirements and Objectives (DRO) for the aerodynamic design of this vehicle. The geographical features of the Galeras Volcano (4276 m a.s.l.), located in San Juan de Pasto - Colombia ($1^o13'31''N, 77^o21'68''W$) were selected [5, 6]. Hence, the URCUNINA-UAV must be able to fly up to 4300 m a.s.l. i.e, it requires a high service ceiling. At this great altitude, the wing lift is reduced due to the rarefaction of the air. Therefore, the choice of the wing airfoil was emphasized to obtain a sufficiently high lift coefficient (C_L). A powerful propulsion system is also required because of the mass flow rate decrease at the operating altitude. Thus, the selected engine/propeller must reach this performance requirement, keeping sufficient Thrust to Weight Ratio (T/W) during each phase of the mission profile. Fig. 1 shows the Galeras Volcano map risk, which has a radius of high threat zone (red zone) of 11 Km, a radius of medium threat zone (orange zone) of 40 km and a low zone threat zone of 100 km (yellow zone) [6].

Fig. 1 Galeras Volcano risk map.

The URCUNINA-UAV is constituted by the launch and recovery systems, i.e. a catapult for take-off and a parachute as a vertical landing device. Likewise, the communications equipment of flight control and the equipment to distribute the data obtained by the payload are included. The aboard systems includes: Auto-pilot, several gas sensors, including a miniature mass spectrometer, GPS sensors, photo-video cameras with infrared system and a data link, as communication system to control the information obtained from the payload [7].

Due to the fact that real environmental conditions of volcanoes are difficult to be represented in wind tunnel experiments, the numerical and experimental studies focused on assessing the Reynolds number similarity. In this way, a scale model of the URCUNINA-UAV was designed and manufactured. Specific characteristics were observed, analogous to the aerodynamic behavior of the actual aerial vehicle, such as soft-stall at high angles of attack and high lift coefficient.

As an additional support to this research, Bravo-Mosquera et al [8] presented more specific details of the URCUNINA-UAV design in this sort of specific mission.

2 Design procedure

The conceptual design of the URCUNINA-UAV was conceived from potential opportunities in the future market. Having derived the mission requirements from these predicted opportunities, the search for the technology with respect to the imposed flight conditions initiated. This custom design methodology was founded upon methodological proposals developed by Roskam [9], Raymer [10], Nicolai [11] and Austin [12].

The URCUNINA-UAV design procedure was divided into three main stages (Fig. 2). The first refers to the definition of design parameters, which include operational requirements related to performance characteristics, and payload weight (Wp). An extensive research was conducted about photographic and environmental UAVs, forming a database with 20 UAVs to analyze their main design features. To this end, a multidisciplinary design optimization (MDO) tool was developed, which integrates the concepts of statistical entropy and quality function deployment (QFD). This tool is used to identify the new design concepts that have been introduced in the market by each vehicle. Furthermore, even within the first stage, an initial weight estimation of the UAV was performed, ending with the constraints analysis to choose the propulsion system. The second stage refers

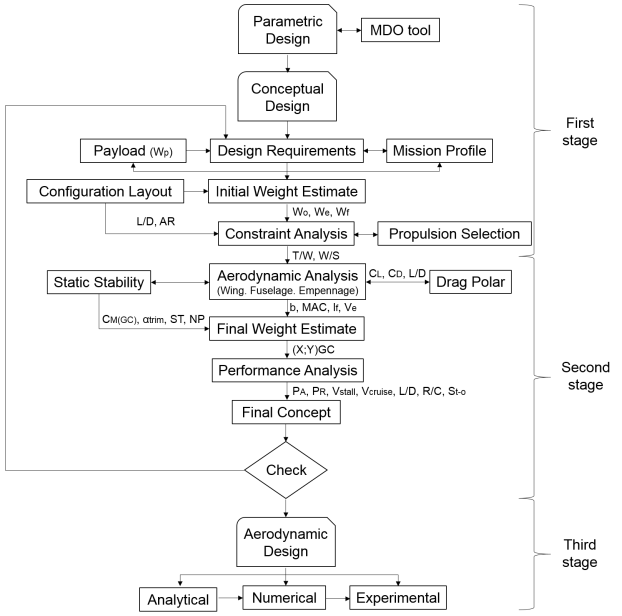

Fig. 2 Design methodology flow chart [8].

to the preliminary estimations regarding the basic aerodynamic, geometry, weight, stability and performance parameters. Once the aerodynamic design is established, the final stage consists of CFD simulations, and wind tunnel experiments using a scale model of the URCUNINA-UAV, in order to determine the aerodynamic coefficients to predict the vehicle behavior prior to manufacturing. Figure 2 shows the logical process carried out during the conceptual design phase.

2.1 Design requirements and objectives

The design process started defining the requirements and objectives (DRO) of the URCUNINA-UAV based on the mission profile established. The following operational requirements were defined: take off altitude, service ceiling, operational altitude, endurance and payload. These flight requirements are generals and describe the needs of the aircraft. Each parameter showed in table 1 is based on parametric studies and the mission of the URCUNINA-UAV.

The proposed mission profile to carry out superficial research of volcanic environments is presented in Fig. 3.

Table 1 DRO of the URCUNINA-UAV [8].

Requirement	Performance
Take-off altitude	2527 m
Operational altitude	4500 m
Endurance	4 h
Payload	4 kg
MTOW	15.64 kg
Monitoring velocity	$\approx$ 20 m/s
Cruise velocity	$\approx$ 28 m/s

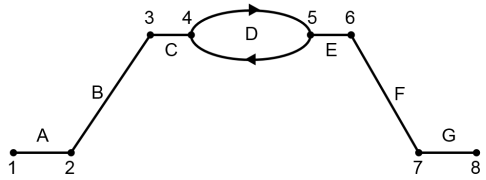

Transition points — 1: Engine ignition; 2: Take-off; 3: Operational altitude point; 4: Start volcano monitoring; 5: End volcano monitoring; 6: Start descent; 7: Landing; 8: Stop engine. **Flight stage** — A: Take-off run; B: Climb; C: Cruise out; D: Volcano monitoring; E: Cruise back; F: Runway approach; G: Landing.

Fig. 3 Mission profile of the URCUNINA-UAV [8].

2.2 Final concept

After design iterations, the final concept is an inherently stable UAV with a total endurance greater than 5 hours, MTOW = 15.5 Kg, service ceiling = 5000 meters, stall speed = 12 m/s, operational speed = 21 m/s, EPPLER 423 wing airfoil and NACA 0012 tail airfoil. The 3 views and isometric view of the final prototype of the URCUNINA-UAV are shown in Fig. 4.

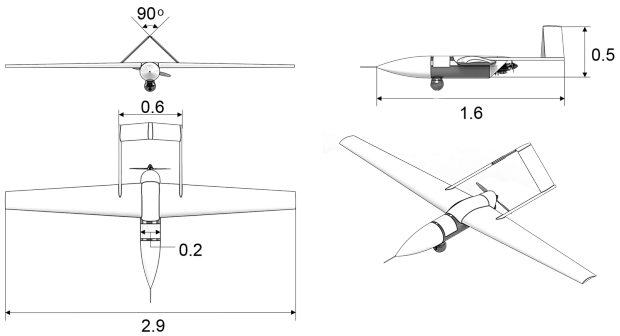

Fig. 4 URCUNINA-UAV [8].

Further detailed information about the conceptual design, performance and stability analysis of the URCUNINA-UAV are reported in [8].

3 CFD simulations

The CFD analysis was carried-out with the commercial code Ansys-CFX [13]. The analysis was based on resolving Reynolds-Averaged-Navier-Stokes (RANS) equations, coupled with the Shear Stress Transport ($k-\omega$ SST) turbulence model. The Shear Stress Transport turbulence model was used since it models typical low Reynolds aerodynamic problems [14].

This section aims to compare numerical results with the experimental results from wind tunnel tests. The simulations were performed at the altitude of the wind tunnels location, using a half scaled model (1:2.4) of the URCUNINA-UAV. Then, the main dimensions of the scale model are: MAC = 0.11 m, b/2 = 0.6 m and total length = 1.2 m as can be seen in fig. 5.

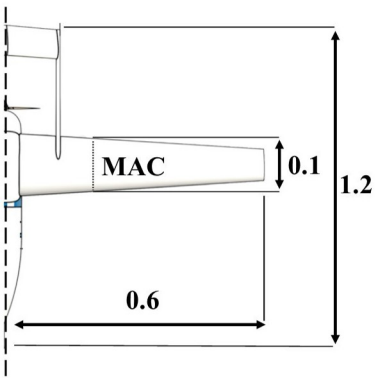

Fig. 5 Main dimensions of scale model.

3.1 Numerical approach

The dimensions of the computational domain and the boundary conditions were adjusted to the characteristics and location of the closed wind tunnel used for the experiments [15].

A grid independence study was carried out, to ensure that the grid refinement does not affect the solution. This study gave the size of the elements of the grid with the lowest computational cost. As can be seen in Fig. 6, for zero angle of attack, from 8×10^6 elements, the C_L coefficient no longer changed their values considerably. In this way, the distance for the first layer of cells away from the wall was set in $y = 1e-4$, resulting in a $Y^+ \approx 1$.

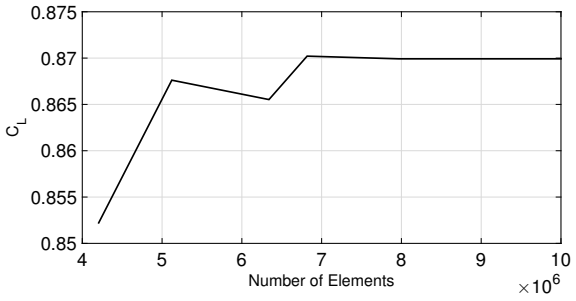

Fig. 6 Mesh independence [8].

Unstructured meshes with tetrahedral elements were created for the whole domain, however, structured meshes were created near the wall with the aim of capturing the boundary layer effects. Figure 7 shows the final grid configuration and some refinement parts on the UAV surface.

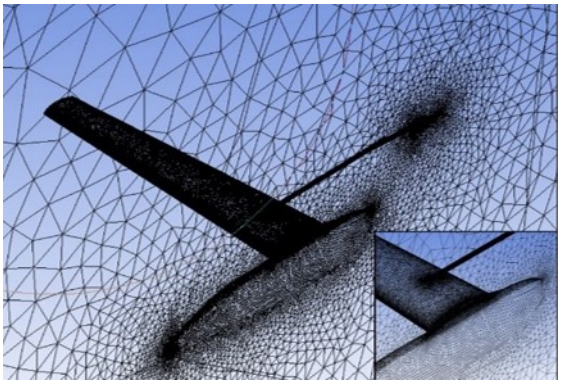

Fig. 7 Grid details of the simulations.

3.2 Boundary conditions

Pressure and temperature were calculated with the ISA (International Standard Atmosphere) at an altitude of 856 MSL, which is the altitude of the Aircraft Laboratory of the São Carlos Engineering School, University of São Paulo, Brazil. Velocity inlet was set at 29 m/s, which represents the project Reynolds number approximately equal to 2.15×10^5 based on the MAC. Inlet turbulence intensity equal to 1% and turbulence eddy viscosity equal to 0.2 were also selected. Outlet velocity was set without pressure gradient difference at outlet region. Symmetry condition was imposed in the half of the longitudinal plane of the model. The walls of the virtual

wind tunnel were treated as Free-slip wall (Ideal wall), because wall corrections were considered for the experimental results. The UAV model was treated as a No-slip wall. A wide range of angle of attack was examined, from $\alpha = -6^o$ to $\alpha = 20^o$, revolving the model around the pitch axis.

3.3 Pressure contours

Figure 8 show the streamlines and pressure contours on the URCUNINA-UAV at $\alpha = 0^o$, 8^o, 14^o (pre-Stall angle) and 20^o (stall angle), respectively. As can be seen in fig. 8a and fig. 8b, the fluid does not present detachment. On the other hand, in fig. 8c and fig. 8d are observed fluid separation on the wing/fuselage junction and wing-tail boom junction, this occurs by the stall effect presented at this angles of attack.

4 Wind tunnel experiments

The experiments were carried out in two stages. First, the acquisition of the aerodynamic forces was conducted in a closed-circuit wind tunnel that has a test section of 1.30 x 1.70 x 3.00 m [15]. The maximum velocity achieved is about 40 m/s and the turbulence level is 0.21%. On the other hand, flow visualization experiments were undertaken in a blower wind tunnel with an open working section of 0.8 x 1.05 m. The operating velocity range is from 10 to 30 m/s. Both tunnels are located at the laboratory of aerodynamics (LAE) of the São Carlos School of Engineering - University of São Paulo (EESC-USP), Brazil.

The Cliever CL2 pro plus 3D printer was used to manufacture the scale model (1:2.4) of the URCUNINA-UAV (Fig. 5), which use Polylactic Acid (PLA) as building material. Eight pieces were printed to complete the model using an internal structure of honeycomb type. The size of honeycomb in the wing is much denser than the fuselage, in order to the wing be stiffer. Figure 9 shows the manufacturing process and the pieces of the model.

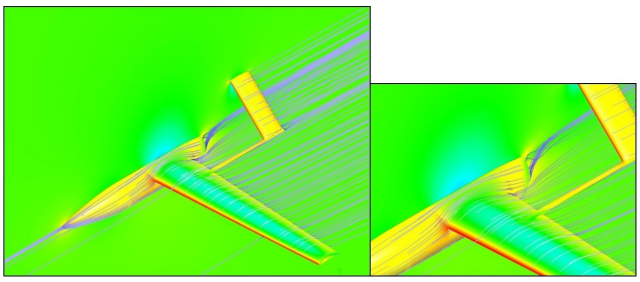

Fig. 8a. $\alpha = 0^o$.

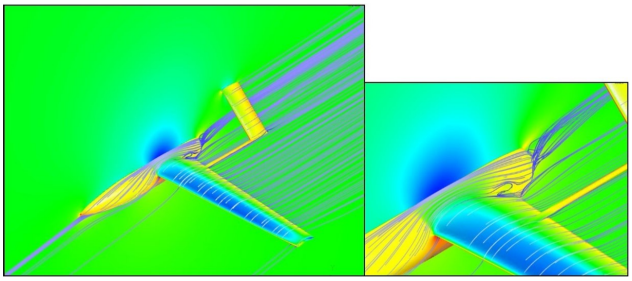

Fig. 8b. $\alpha = 8^o$.

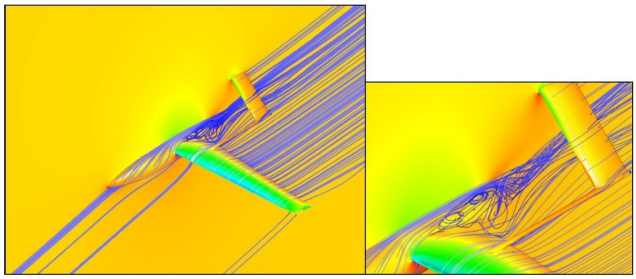

Fig. 8c. $\alpha = 14^o$.

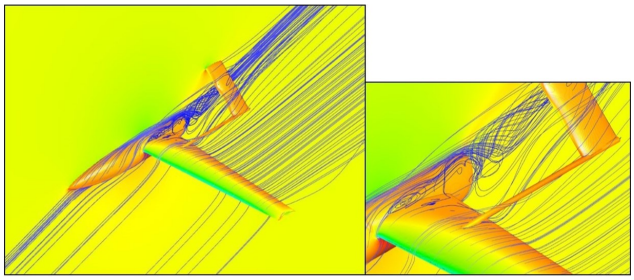

Fig. 8d. $\alpha = 20^o$.

Fig. 8 Pressure contours and streamlines on the URCUNINA-UAV.

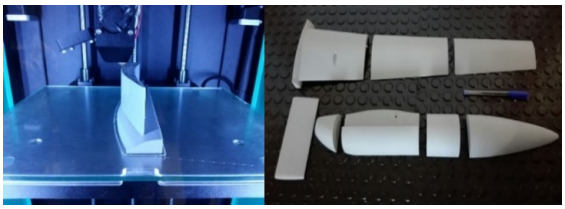

Fig. 9 3D printed Model [8].

4.1 Balance experiments

The aerodynamic balance measures two key forces on the model: lift and drag. The uncertainty of the forces measured with the aerodynamic balance was $\pm$ 0.01 N. It is connected in a conditioner amplifier installed in a microcomputer. Data reading is through a computational tool developed in the application "Lab View" (National Instrument), which was set to take 5000 samples with a frequency sample of 500 samples per second. Dynamic pressure was measured with a micro manometer which has an uncertainty of $\pm$ 0.1 Pa. The uncertainty of measure of the chord and the wing span was of $\pm$ 0.001 m in each of them.

The total frontal projected area of the experimental model was 0.035 m^2, which corresponds to 1.54% of the total area of the wind tunnel cross section. Therefore, as this ratio is less than 8%, blockage phenomena can be neglected. Figure 10 shows the final scale model of the URCUNINA-UAV at the wind tunnel test section.

Fig. 10 Wind tunnel test.

4.2 Flow visualization

The flow visualization technique used is known as surface oil-flow (Fig. 11), which enables the observation of the boundary layer flow in wind tunnel easily and quickly. In this technique the model surface is coated with a mixture of a vegetable oil and fine pigment, indicating the pattern of the flow on the surface. The technique allows the observation of the lines of separation and reattachment of the flow.

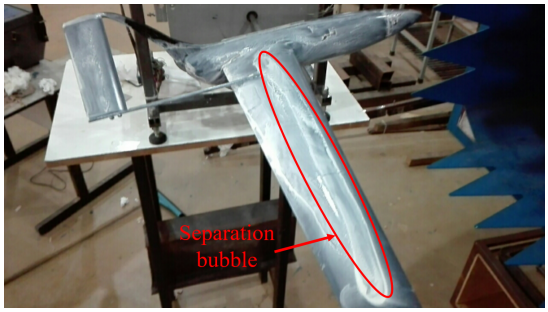

Fig. 11 UAV in the blower wind tunnel.

5 Results

In this section, the experimental and numerical results of the UAV are presented. First of all, the experimental results of the LSB phenomena are discussed. Once obtained the corresponding boundary layer transition, results are compared to numerical ones.

Figures 12 and 13 show the C_L vs α and C_D vs α curves obtained experimentally. There is a severe decrease of lift and increase of drag between $\alpha = 3^o$ to $\alpha = 11^o$. This is due to the presence of a laminar bubble on the upper surface. On the other hand, above $\alpha = 11^o$, the kinetic energy of the fluid increases and promotes the transition from laminar to turbulence flow prior to the separation of the boundary layer and the aircraft behavior become back to the normal behavior. Indeed, through the visualization experiments, the presence of a bubble in this range of angles of attack was verified, e.g. at $\alpha = 0^o$, a bubble is formed approximately at 25% of MAC with a length of 3 cm approximately, (25% of MAC), as can be observed in Fig. 11.

To avoid the formation of the bubble, two alternatives were considered. First, the free-stream velocity was increased, raising the Reynolds number. On the other hand, a roughness at 25% of MAC was set. Both of them avoided the LSB and there was no such abrupt decrease in C_L values in the range $3^o \leq \alpha \leq 11^o$, (see fig. 14 and fig. 15). This occurs on account of in both cases the transition is before the separation point. In the first case, due to the increase of the flow ki-

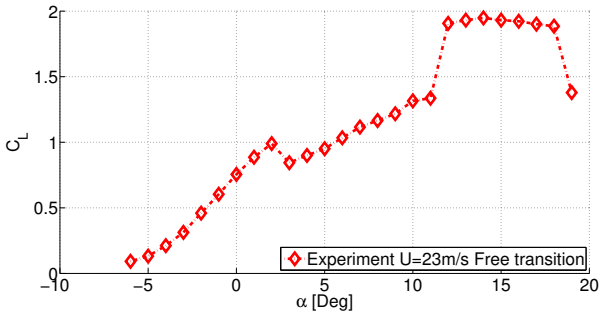

Fig. 12 Lift coefficient with LSB.

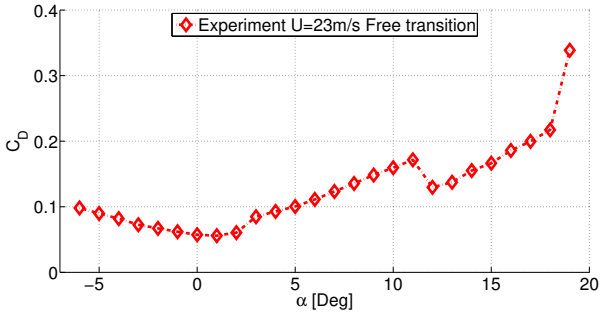

Fig. 13 Drag coefficient with LSB.

netic energy, and on the second case, due to the forced transition before the separation.

To define the roughness, the bubble feature observed in flow visualization at 11^o was considered. It was defined the separation point and the roughness was located before to guarantee the transition. Figure 16 shows XFOIL simulation at $Re = 1.5$ x 10^5, $N_{crit} = 9$ and $AoA = 0^o$ with free transition and forced transition at 25% of MAC, which represents the trip on the real model. With forced transition model, the pressure distributions does not present bubble phe-

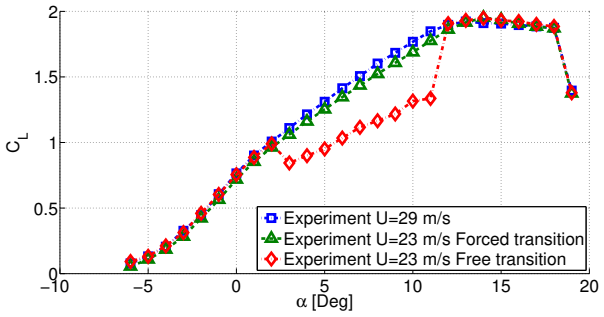

Fig. 14 Lift coefficient with transition methods.

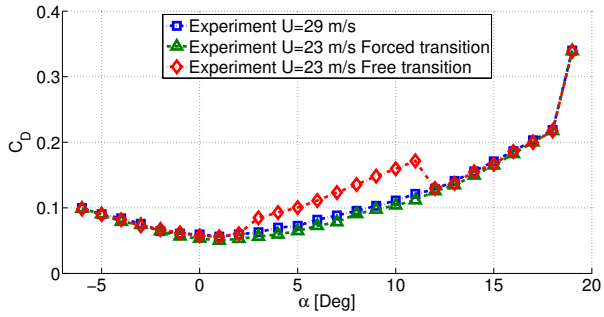

Fig. 15 Drag coefficient with transition methods.

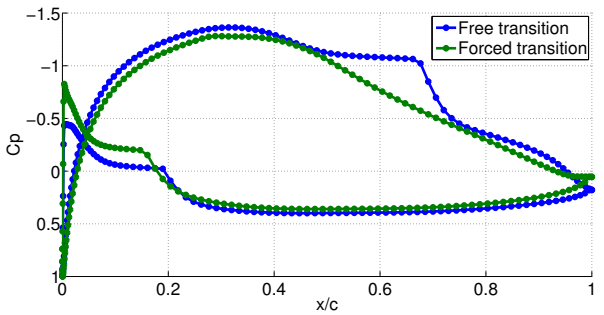

Fig. 16 Pressure distribution with free and forced transition.

nomena, however reduce the suction peak.

According to the results of Fig. (17), from $\alpha = 0^o$ to $\alpha = 12^o$, on the linear behavior of the curves, note that the slope $(\partial C_L/\partial_\alpha)$ of the two curves are similar, in spite of obtaining variations for C_L values at zero angle of attack. The numerical and experimental curves presented similar behavior for all angles of attack evaluated. However, the curves presented similar pre-stall angles, $\alpha = 13^o$ for experimental and $\alpha = 14^o$ for the numerical curve. This represents a favorable behavior in the proposed mission, because it allows recovering the UAV at high angles of attack, before reaching the strong stall. This typical behavior is caused by the wing airfoil at high turbulent flow, which contributes to maintain a stable performance in the long run.

Figure 18 shows the results of the drag coefficient. As it was expected, an excellent approximation of the numerical results with the experimental ones was obtained, where the C_D values at zero angle of attack were 0.048 and 0.053 respectively.

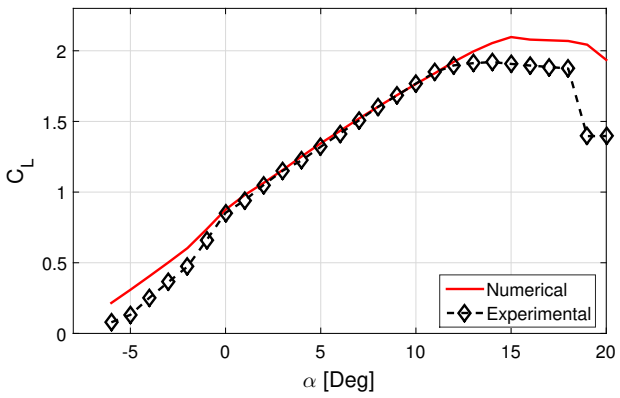

Fig. 17 Lift coefficient.

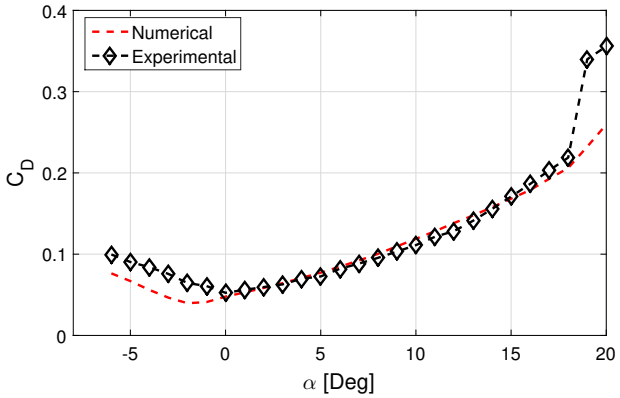

Fig. 18 Drag coefficient.

For negative angles, the numerical and experimental curves presented an abrupt decrease of C_L, which produced an increase in the C_D. This is caused by the great curvature of the wing airfoil. However, even in negative angles, the UAV generates sufficient C_L to maintain its flight.

Figure 19 shows the aerodynamic efficiency curves versus angle of attack. It was observed that for the numerical curve the maximum value of the lift-to-drag ratio were set at $\alpha = 0^o$, and for the experimental curve at $\alpha = 5^o$. Both curves presented the same value of aerodynamic efficiency, being L/D = 17.7. On the other hand, figure 20 relates the URCUNINA-UAV drag polar for the entire design process of the aircraft. It was observed that the numerical and experimental values were close. For the sake of argument, it can be concluded that all the aerodynamic analysis for evaluating the conceptual design of the

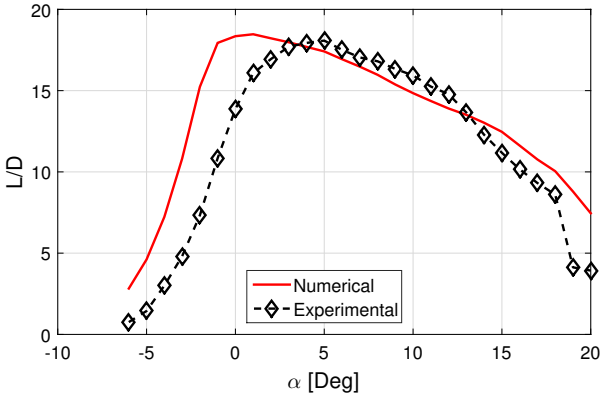

Fig. 19 Lift to Drag ratio.

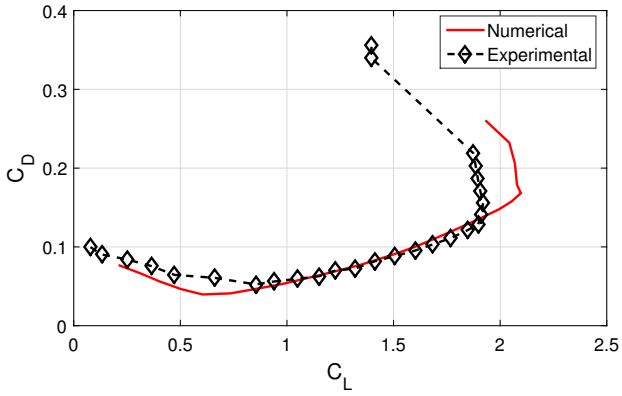

Fig. 20 Drag polar.

URCUNINA-UAV were performed successfully, because specific characteristics were adjusted to the mission requirements, such as high aerodynamic efficiency and soft stall.

Finally, in Table 2, the main results of the total aerodynamic design process are summarized. As a conclusion, the numerical and experimental results were well developed, since the results match closely.

Table 2 Comparison of aerodynamic coefficients.

Aerodynamic parameters	Numerical	Experimental
Maximum C_L	2.09	1.92
α for C_{Lmax}	15^o	14^o
C_L at zero α	0.87	0.85
C_D at zero α	0.048	0.053
$\partial C_L/\partial_\alpha$	0.083	0.081
Maximum L/D	17.7	17.7
α for $(L/D)_{max}$	0^o	5^o

6 Concluding remarks

The conceptual design and its respective aerodynamic analysis of a new concept of low-cost UAV intended to be used in one of the many methods for monitoring an active volcano have been developed.

The results obtained with computational, and experimental methods enriched the research exercise during the design of the URCUNINA-UAV. In this way, it was possible to analyze and validate the main findings, which are summarized in the following statements:

- The SST turbulence model was efficient in predicting the aerodynamic behavior of URCUNINA-UAV with sufficient precision, obtaining C_L and C_D values very close to those found in wind tunnel testing.
- Wind tunnel tests corroborated data showing that the URCUNINA-UAV is a promising design and would achieve the mission successfully. The C_L requirements for the mission were accomplished and the drag values obtained were close to expected. As a result, a stable and high lift, low drag UAV was obtained.
- High-lift low Reynolds number airfoils present grater advantages in both civil and military applications, however they are liable to present bubble phenomena due to their laminar boundary layer, then it is important to analyze completely the behavior of the wing or airfoil in order to know in which conditions of angle of attack, velocity and turbulence intensity the aircraft could operate. In conditions in which the bubble is formed, the aircraft could not be operated.
- To improve the analysis of the actual-environmental conditions above a volcano, free disturbance and unsteady flow effects must be evaluated. However, the numerical and experimental results presented in this research are promising to complete the URCUNINA-UAV mission.
- As for the resulting UAV, all the analysis was limited to the conceptual and aerodynamic design phase, this UAV concept can serve as a base for future detailed design studies, such as structural analysis, sizing of control surfaces, dynamic stability, among others.

References

[1] Nonami K. Prospect and Recente Research and Development for Civil Use Autonomous Unmanned Aircraft as UAV and MAV. *Journal of Systems Design and Dynamics*. Vol. 1, pp. 120-128. 2007.

[2] Tupper A, Carn S, Davey J, Kamada Y, Potts R, Prata F and Tokuno M. An evaluation of volcanic cloud detection techniques during recent significant eruptions in the western 'ring of fire'. *Remote Sens. Environ*. Vol. 91. No. 1. pp. 27-46. 2004.

[3] Johnston D, Bebbington M, Lai C, Houghton H and Paton D. Volcanic hazard perceptions: comparative shifts in knowledge and risk. *Disaster Prev. Manag*. Vol. 8. No. 2. pp. 118-126. 1999.

[4] Pyle D, Mather S and Biggs J. Remote Sensing of Volcanoes and Volcanic Processes: Integrating Observation and Modelling - Introduction. *Special Publications*. Vol. 380. No. 1, Geological Society, London. pp. 1-13. 2013.

[5] Cortés G and Raigosa J. A synthesis of the recent activity of galeras volcano, Colombia: seven years of continuous surveillance, 1989-1995. *J. Volcanol Geotherm Res*. Vol. 77. No. 1. pp. 101-114. 1997.

[6] Ordón M, Cepeda H, et al. Morphological changes of the active cone of galeras volcano, Colombia, during the last century. *J. Volcanol Geotherm Res*. Vol. 77. No. 1. pp. 71-87. 1997.

[7] Werner-Allen G, Lorincz K, Johnson J, Lees J and Welsh M. Fidelity and yield in a volcano monitoring sensor network. *7th symposium on Operating systems design and implementation*. USENIX Association, California, United States of America. pp. 381-396. 2006.

[8] Bravo-Mosquera P D, Botero-Bolivar L, Acevedo-Giraldo D and Cerón-Muñoz H D. Aerodynamic design analysis of a UAV for

superficial research of volcanic environments. *Aerosp. Sci. Technol*. Vol. 70 (Supplement C) pp. 600-614. 2017.

[9] Roskam J. Airplane design: Parts I through VIII. *DARcorporation*. 1997.

[10] Raymer D. Aircraft design: A conceptual approach. *AIAA education series*. 1999.

[11] Nicolai L and Carichner G. Fundamentals of Aircraft and Airship Design. *American Institute of Aeronautics and Astronautics*. 2001.

[12] Austin R. Unmanned Aircraft Systems: UAVs Design, Development and Deployment. Vol. 54. 2011.

[13] CFX, 14.5 theory guide of ANSYS CFX 14.5, ANSYS Inc.

[14] Steed R G. High lift CFD simulations with an SST-based predictive laminar to turbulent transition model. *AIAA Journal*. 864. 2011.

[15] Santana L, Carmo M, Catalano F and Medeiros M. The update of an aerodynamic wind-tunnel for aeroacoustics testing. *Journal of Aerospace Technology and Management*. Vol. 6. No. 2, pp. 111-118.

7 Contact Author Email Address

mailto: pdbravom@usp.br

Copyright Statement